The swell dynamics and their implications over Africa: significance to climate change and forcing

Abstract

There is a growing interest in climate dynamics as the quantity and quality of new observational and theoretical applications are increasing. The ideas involved in understanding large-scale atmosphere-land-ocean dynamics and their interactions continue to hold special fascination because of their central importance for both theoretical and practical applications. This paper presents a theoretical assessment of the African swell dynamics imploring atmospheric formulation. Africa exhibits substantial inter-annual and inter-decadal climatic variability due to cyclone activity, storm surges and sea waves. Most of these surges and corresponding swell trains form over the tropical environment as easterly waves propagate westward across the Indian Ocean primarily between 10° and 20° S, termed source region. Localized sea surface temperatures (SSTs) and ocean upwelling play a vital role to provide moist enthalpy to power the surges. Also, multi-decadal variations in major wave activity are associated with SST changes in the Atlantic because tropical North Atlantic correlates positively with major hurricane activity. A key remote factor is temperature variability in the central and eastern equatorial Pacific associated with El Niño Southern Oscillation. The continuous erosion, perennial ocean surges, coastal swells and associated flooding due to the wave energy and its pounding effect are of great concern. Just like in most parts of the world where development of these systems is critical, they need to be closely watched particularly over southern Africa.

Key Words: climate dynamics; swell train; source region; wave energy; ocean surge.

1. Introduction

Africa experiences a wide variety of climate regimes and is one continent strongly affected by the subtropical anticyclonic belts and has extensive areas of tropical-subtropical climates. Changes in climate dynamics and variability are likely to exacerbate the existing problems due to episodic wave events that occur with little advanced warning [1]. These impacts are likely to affect many different aspects of the world's environments. Year-to-year variations in topical cyclone (TC) numbers are great, and in many regions strongly linked to El Niño Southern Oscillation [2]. Also, regions of wave activity may increase poleward as a result of increasing sea surface temperatures (SSTs), sea level rise and ocean upwelling. It is clear that any substantial changes in numbers or fatalities of these events have significant consequences in the active and/or vulnerable regions during periods of wind disturbance, storm surge, cyclone activity and/or damaging floods. For example, southern east Africa –including the island of Madagascar appears to be influenced by SST changes over much larger regions [3], and references therein]. The region is frequently affected by cyclonic and other significant weather events [4] that unleash large wave events over land [1] between December and March. Majority of these TCs track south-westerly away fro the mainland and back towards the Indian Ocean. According to Mather and

Stretch [1], these cyclones sometimes remain semi-stationary south of Madagascar that cause the biggest swells in the region. The southern part of Madagascar also appears to be well-positioned to receive strong south-westerly swells from these systems as they move over the ocean [5].

The northwest coast often experience mid-latitude depressions that track across the North Atlantic [6] –the region with a wave activity subject to a high seasonal variation and enhances during the northern-hemisphere winter. Similarly, West-Africa receive north-westerly swells from the North Atlantic during the northern winter and the occasionally long-range swells from the South Pacific during the southern winter. On the other hand, east Africa is often affected by locally-generated wind seas, together with the south (south-easterly) swells from mid-latitude depressions that would have otherwise occurred or propagate over the South West Indian Ocean (SWIO). One significant difference between the South Indian Ocean and the South Atlantic Ocean is that the former is much larger and allows the nature of the Indian Ocean High (IOH) to be more modified [7]. According to the author, the IOH is not a single steady synoptic entity, and tends to slowly move eastwards across the South Indian Ocean and often splits into two waves, particularly with a strong depression poleward and the transition from one cell to the next that provides the trickiest navigation dilemma.

The interplay between the atmosphere, land and oceans driving these systems is extremely complex. Indeed interactions between the waves and currents induce change in the wave direction [8], and references therein. Interactions can result in large variations in weather and/or climate regime spanning to seasons, decades or centuries. Understanding the root causes of these changes and the perceived value of seasonal prediction is vital, given the overwhelming importance of the timescales of climate information and adaptive responses [9].

Although advances to understand these complex mechanisms and how they may influence future climate variability are made, this is a critical area requiring further research [10]. For example, projecting future climate evolution needs some kind of mathematical- or physical approach to understand and/or model. As such, climate scientists try to tackle these issues by understanding the link between various factors that relate air movement and clouds, heat and temperature, rainfall and cloud formation, pressure changes and wind field. One application is the use of existing mathematical laws (the so-called atmospheric equations) to understand the underlying physical problems. Fundamental laws of fluid dynamics and thermodynamics governing atmospheric behavior are expressed in terms of partial differential equations involving the field variables as dependent or independent variables in space and time. These are basic laws of motion derived from the same equations governing all classical fluid dynamics.

This paper aims to understand the status and evolution of the swells and their influence on the African climate variability. We address this on the issues of geophysical fluid dynamics applying some fundamental atmospheric equations. The main objective is to analyze the swell trains as a possible aid to theoretical and/or operational forecasting. The paper also highlights on interannual and intraseasonal variability in the wave activity, including links to

large-scale phenomena such as El Niño Southern Oscillation (ENSO), SSTs and the quasi-binneal oscillation (QBO). Also described are some characteristics demonstrated about African storms and global wave environments.

2. Wave climates and swell generation

2.1 Major global wave environments

There are significant patterns of wind belts and oceans identified globally, that cause the major wave climates. The largest of which are associated with gale force winds of the sub-polar and temperate latitude regions, characterized by the occurrence of westerly winds and frontal activity [11]. According to the author, these occur in latitudes around 60°S in the southern hemisphere (SH), whereas in the northern hemisphere (NH) they occur in the "roaring forties", 40–60°N. The trade wind belts are characterized by strong persistent winds and maintain the swells, although they are rare in the doldrums of equatorial latitudes. Tropical cyclones (also described in different nomenclature in different places) significantly influence waves on many tropical coasts, but do not occur within 5°N–5°S region of the equator. Figure 1 illustrates the major areas of influence by these systems. The five broad wave environments have been recognized as:

i) Storm wave environments: occurs where gales generate short high-energy waves of varying direction.
ii) East coast swell: consist of weaker swell, amplified by local wave generation
iii) West coast swell: occurs on coasts experiencing low long-swell waves of consistent direction with rare storms
iv) Monsoon influence environments: experience a reversal of principal wind wave directions, and
v) Protected sea environments: large water bodies in which wave generation is localized rather than swells from the large ocean basins.

As shown in the figure, the east and west coasts are often affected by the east and west swells, with the southeast also subject to the TCs from the SWIO tracking westwards. Moving further east towards south Asia, the region is subject to monsoon influence which sometimes reach Africa via the so-called Great Horn of Africa.

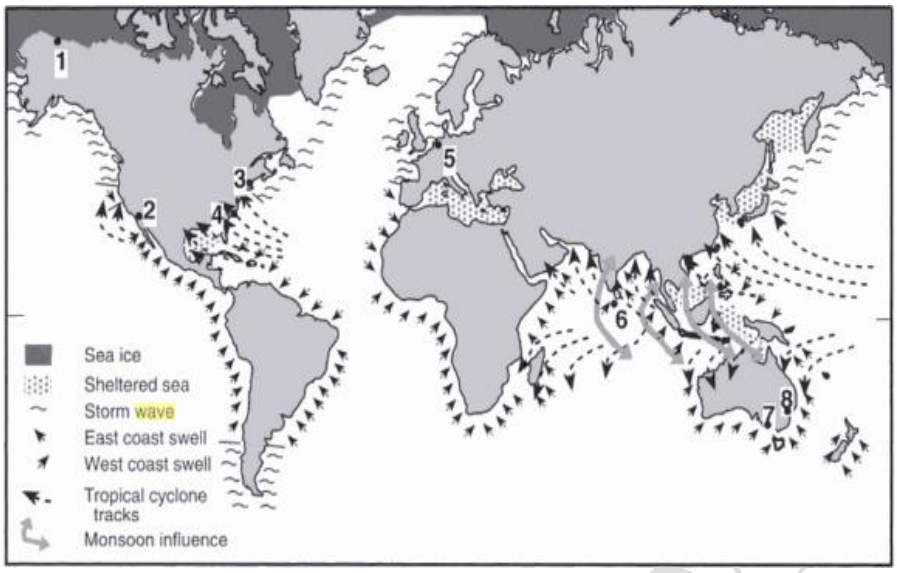

Fig. 1. Major wave climates [11]

2.2 Wave generation and swell trains over Africa

Africa is generally characterized by stark climatic contrasts, significant inter-annual and inter-decadal climate variability [12]. An upper anticyclonic circulation continues aloft in both hemispheres all year round so that a high zonal index prevails. The continent is surrounded by the Atlantic and Indian oceans that play an important role in its climate. Generally, the ocean surface is either 'wind sea' or swell dominated. The surface displays a combination of wide gravity waves with varying amplitudes and frequencies. These are swell waves which can propagate out of their generation zones and travel longer distances without significant attenuation [13]. Because they can propagate to distant areas without much disturbance, they contain a significant nature and wind intensity along, making them precursors to various atmospheric phenomena such as storms, TCs and other large-scale sea breeze systems. A preexisting low-level cyclonic disturbance is one necessary condition for a TC development, a vast majority of which form over tropical environments [14].

Almost all swell trains reaching Africa are generated from the southern oceans' storms with less frequency coming from the northern oceanic areas. Occasionally, storms approach from the east driven by frontal systems over the SWIO (Fig. 2). The figure shows regions of active swells across the globe, indicating that oceanic areas are the most active source regions (SRs). Most of these occur over the warm waters of the Indian Ocean and propagate westwards, where they sometimes result in devastating impacts over land. Adverse conditions are often expected offshore, especially during the summer season. Short waves comprising local seas and swells are generated mainly by passing frontal systems (low pressure systems) from the Atlantic, cut-off low-pressure systems and occasional TCs over Mozambique Channel [15]. According to Gray et al. [16], about 87% of TCs develop between latitudes 20° north and south, two thirds of which

develop in the NH, and twice as many in the eastern than western hemisphere.

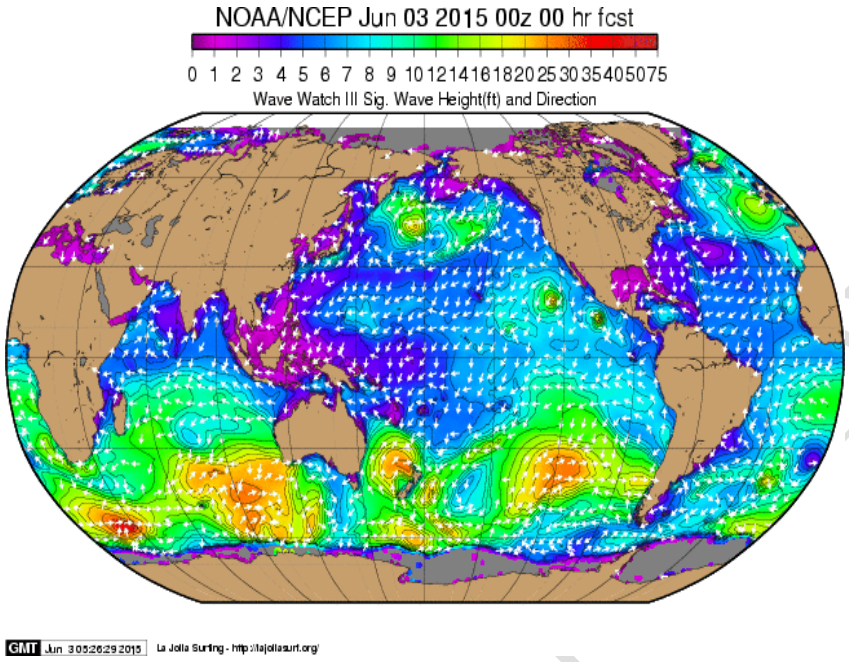

Fig. 2. Global Swell model, showing swell generation areas in the main oceanic areas. (http://www.surftrip.com/surfresources/swellmodels/swellmodels.html).

Consistent with figure 2, figure 3 also shows global cyclone tracks, again indicating the Indian and Pacific Oceans as active SRs of cyclone activity. Normally, the surges tend to move westwards, curving from the equator, sometimes comprising of large rotating thunderstorm masses [17]. Quite often, it has been observed that the swells arrive from the oceanic region south of 35 °S – a region defined as the Southern Ocean, and grow significantly under the influence of local wind conditions [13]. Mid-latitude waves are refracted equatorward, due to large index values resulting from diminishing westerly winds [18]. Unlike in the NH where the Coriolis force deflects winds to the right, winds are deflected to the left in the SH. Coriolis force helps to spin the aggregation of thunderstorms into a characteristic spiral circulating winds. The basic horizontal balance between a TC above the boundary layer is due to the sum of the Coriolis 'acceleration'

and the centripetal acceleration balanced by the pressure gradient force [19]. Coriolis acceleration is the product of horizontal air parcel velocity and the Coriolis parameter f ($f = 2\Omega \sin\phi$, where Ω is earth angular velocity and ϕ is latitude), which becomes zero at the equator and 2Ω at the poles.

Recent studies indicate that sea state along the coastal Indian Ocean is significantly influenced by the swells which are predominant during southwest monsoon [13,20]. For example, the World Meteorological Organization (WMO) report indicate that there was near-average tropical storm activity in the SWIO during the 2001-2010 decade; the most active season was observed in 2009 with a total of 16 tropical storms and 7 cyclones (Fig. 4).

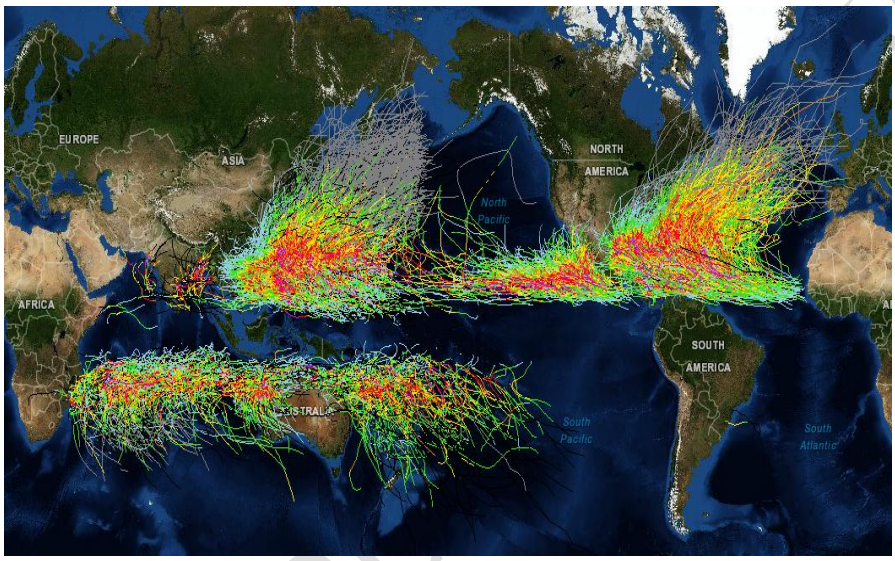

Fig. 3. Global cyclone tracks (Figure curtsey of: https://geozoneblog.files.wordpress.com/2014/05/globalwrappedclipped.png)

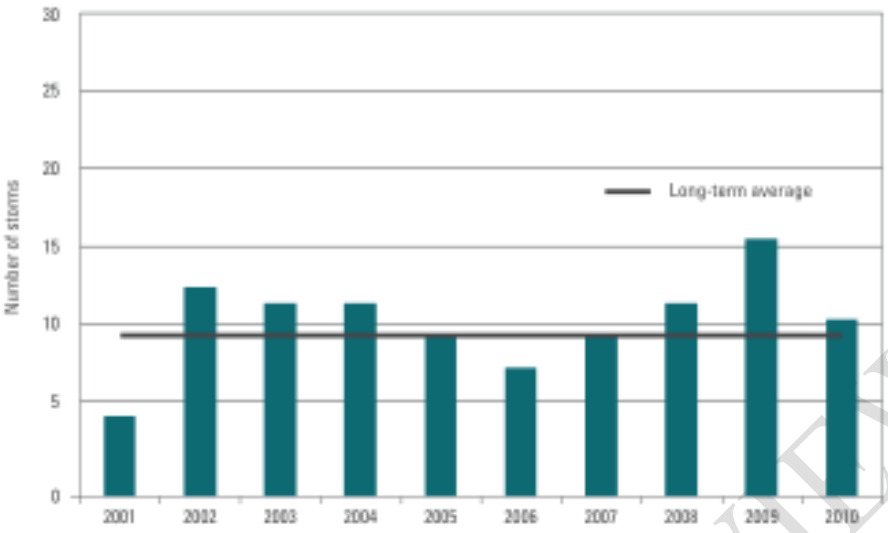

Fig. 4. Statistical storm number over the SWIO in the 2001-2010 decade. (Source: WMO, [2])

Generally, waves travel from the same direction in groups as a collection of sinusoids with different periods. The generation and growth of the waves is primarily dependent on wind duration, speed and fetch [13]. This is an important concept that determines the rate at which energy propagates both spatially and temporally [21]. However, even in the absence of significant wind disturbance, there can still exist waves of varying wavelengths over the water surface. A swell generation is largely governed

by the deep water dispersion [22] given by:

$$c_g = \frac{gT}{4\pi} \quad (1)$$

where c_g is group velocity, T is wave period and g is gravitational field strength. Nevertheless, even after generation, some processes can still operate in the wave evolution [6], such as: i) refraction of waves related to ratio of current gradient to wave group velocity; ii) advection of wave action by the current vector; iii) change in wave number and group speed and iv) local influence of wind vector relative to current vector. These can lead to a decrease in the wave steepness and eventually become long-crested swells [23]. The principal fate of a wave depends on the large-scale environment in which it is embedded, its synoptic structure, mesoscale- and convective-scale processes associated with its evolution [24]. Wind-waves generated by intense storms become swells as they leave their generation zone [25,26] and travel very long distances across the ocean basin without much disturbance [13,27]. Wave components with faster wind speed are considered swells, whereas slower ones are taken as wind-seas [28].

The wave train evolution can be expressed [6] as:

$$\frac{dx}{dt} = \frac{\partial \Omega}{\partial k} \quad (2a)$$

$$\frac{dk}{dt} = -\frac{\partial \Omega}{\partial x} \quad (2b)$$

$$\frac{dN}{dt} = 0 \quad (2c)$$

where $\Omega(k,x) = \sqrt{gk} + k \cdot u$ is the dispersion function and $N(k) = \frac{E(k)}{\sqrt{gk}}$ is the wave action, ***k*** is wave vector along the trajectory path and ***u*** is surface current vector. As the waves move towards the ocean boundaries, wind speeds diminish and waves move faster. Eventually they would reach a point when the peak waves have phase speeds larger than the wind and then propagate out of their generation zones as the wave energy ***E(k)*** grow and the peak period increases. Tropical cyclone generated waves are more energetic and usually have catastrophic consequences in many parts of the globe.

2.3. Cyclonic events and associated swell vagaries over Africa

Africa is susceptible to extreme weather events that sometimes cause damages to infrastructure, livelihoods and ecosystems. These events account for the large percentage of natural disaster deaths [29]. For example, during the 1991–2000 period, a number of Africans lost their lives as a consequence of severe meteorological and hydrological events almost doubled [30]. The occurrence of these severe weather events and their resulting disasters is gradually increasing and noticeable signs of the vagaries resulting from global warming and climate changes are evident. Some of the most devastating TCs over the Indian Ocean include Eline-Leon (February 2000), Gloria (February-March) and Hudah (March–April) 2000 which struck Mozambique, Madagascar and other parts of southern Africa, causing severe flooding and about 700 lives lost in Mozambique and millions being displaced. Mozambique experienced the most powerful cyclone of recent time [31].

The WMO also reported that the SWIO turned out to be an active region during the 1999–2000 season due to a high number of cyclone activity and will be remembered for a long time to have the most intense depressions, high winds and severe flooding. For example, cyclone Eline-Leon earned accolade as the longest lived and farthest traveled cyclone on record in the SH [30,32]. Remnants of Eline traversed the subcontinent with torrential rains causing floods further inland, including ephemeral desert rivers [33]. Other typical swells include a series of high waves that broke over La Reunion island in May 2007, resulting in extreme weather events off the southeast coast of the mainland [20]. The waves resulted in numerous damages to property and many lives lost within the neighbouring islands. Just recently, another devastating cyclone Idai developed over the SWIO between Mozambique Channel and Madagascar in March 2019 and caused very catastrophic effect in Mozambique, Malawi and Zimbabwe. A lot of infrastructure and dams were destroyed between March and April, with an estimated $1 billion of infrastructure damage and more than 100,000 homes destroyed according to the United Nations report (https://www.worldvision.org/disaster-relief-news-stories/2019-cyclone-idai-facts).

3. Convective storms

Storms develop over the oceans when a large part of the ocean or sea attains a certain temperature gradient (at least 27^{o}C) from the vertical air motions [34], due to the buoyant or mechanical forces that provide efficient vertical heat

transport, mass and momentum to the rising air. Once this temperature is reached, vast quantities of water are evaporated and the warm air is carried upwards by spiral winds that condense upwards to form huge clouds and develop into a convective system. Convection initiation is linked to mechanisms by which the air is lifted and accelerates upwards, driven primarily by buoyancy [35]. The air experience atmospheric instabilities as it is heated from below while cooling at the top, or when it becomes saturated in the atmosphere. Latent heat plays an important role in the storm growth and energy dissipation. The size of the storm is important because it determines the fetch conditions, together with wind energy and speed. Maximum winds constrain the wave field and its main characteristics [8]. Depending on the amount of energy released and atmospheric instability, the overall process can lead to thunderstorm formation.

Convective storms can take a large variety of forms and scale ranges –from isolated thunderstorms involving a single convective cloud (or cell) to mesoscale convective complexes consisting of ensembles of multicelled systems. Their behaviour is inherently dependent on the environment in which they develop, including thermodynamic stability, vertical wind profiles and mesoscale forcing [36]. Moisture and instability, together with a triggering mechanism are key parameters of deep convection and evolution, followed by a lifting process [37]. Deep convective cells are parent storms for most severe weather events often found in regions such as equatorial Africa, Amazon southeast Asia, Indonesia and northern Australia [38]. Such super cell storms often produce heavy rain, and/or damaging tornadoes. Initiation requires the presence of specific ingredients such as moisture and instability –a source of upward motion and strong vertical wind shear [39]. However, a split may occur so that the storm develops into 2 forms; one moving left and the other moving right. Usually the former dies rapidly while the latter slowly evolves into a rotating circulation with a single updraft core and trailing downdrafts.

3.1. The right-moving storm

Much of the atmosphere-ocean motion is governed by a set of equations known as the Navier-Stokes equations. The equations are used in making weather forecasts, computational analysis as well as ocean current studies. Although there are uncertain details about the equations, they are for most parts accepted as fact [40]. When describing a system, we express simple relationships between relevant variables; and in the present case, express continuity of mass, momentum, potential temperature etc. then eliminate variables to discover wave and diffusion equations as special cases. For example, pressure can be eliminated by differentiating the momentum equation

$$\rho \frac{Dv}{Dt} + \nabla p - \rho \nabla \phi = \mu \nabla^2 v \qquad (3)$$

which consists essentially of integrating round a closed circuit so that the effect of the large potential force ∇_p due to pressure field vanishes identically. This integration round a circuit produces a vector equation for the line integral of velocity, known as *'vorticity'* (a microscopic measure of fluid rotation and a vector field defined as the curl of velocity). Vertical buoyancy gradient can influence the perturbation pressure *p'* field [41], which can be obtained by

taking the divergence of the horizontal momentum equation (3) above:

$$\frac{1}{\rho_0}\nabla^2 p' = -\nabla\cdot(v\cdot\nabla v) + \frac{\partial B}{\partial z} \qquad (3^*)$$

where $B = g\theta_v'/\overline{\theta_v}$. A positive buoyancy anomaly in the upper troposphere and negative anomaly in the lower troposphere produce a positive $\partial B/\partial z$ in the mid-troposphere, thus creating a meso-low ($\nabla^2 p' > 0$). When the environmental wind shear (a small change in the horizontal wind over some vertical distance between two altitudes) is unidirectional, the anticyclonic (left-moving) and cyclonic (right-moving) updraft cores are equally forced.

More often, it is convenient to deal with vorticity than circulation. For example, we use absolute vorticity ω_a and relative vorticity ω_r defined by:

$$\omega_a = \nabla \times U_a \qquad (4a)$$

$$\omega_r = \nabla \times U_r \qquad (4b)$$

where ∇ is the 3-D del operator while U_a and U_r denote the absolute and relative velocities respectively. In Cartesian coordinates;

$$\omega = \left(\frac{\partial w}{\partial y} - \frac{\partial v}{\partial z}, \frac{\partial u}{\partial z} - \frac{\partial w}{\partial x}, \frac{\partial v}{\partial x} - \frac{\partial u}{\partial y}\right) \qquad (5)$$

In most severe storms hitting Africa, the mean flow turns cyclonically with height. The dominance of the right-moving storm can be understood qualitatively by considering the dynamical pressure perturbations. We can define the basic state wind shear vector $\overline{S} = \frac{\partial \overline{V}}{\partial z}$, (assumed to turn clockwise with height) noting that the basic state horizontal vorticity as:

$$\overline{\omega} = k \times \overline{S} = -i\frac{\partial \overline{v}}{\partial z} + j\frac{\partial \overline{u}}{\partial z} \qquad (6)$$

In order to understand the generation of updrafts in the vortices on the flanks of the storm, perturbations are examined on pressure field [42]. For example, the Euler momentum- and continuity equations may be expressed (using Boussineq approximation) as:

$$\frac{DU}{Dt} = \frac{\partial U}{\partial t} + (U \bullet \nabla) = -\frac{1}{\rho_0}\nabla_p + bk \qquad (7)$$

$$\nabla \bullet U = 0$$

where $U = V + k\omega$ is the 3-D velocity, ρ_0 is deviation pressure from the horizontal mean and $b = -\frac{g\rho'}{\rho_0}$ is the total buoyancy, while ∇ is as defined in equation (4) above. It is therefore, convenient to rewrite the momentum equation using the vector identity;

$$(U \bullet \nabla) = \nabla\left(\frac{U \bullet U}{2}\right) - U \times (\nabla \times U) \qquad \text{to}$$

obtain the relation:

$$\frac{\partial U}{\partial t} = -\nabla\left(\frac{p}{\rho_0} + \frac{U \bullet U}{2}\right) + U \times \omega + bk \qquad (8)$$

Taking the curl of equation (7), recalling that the curl of the gradient vanishes, we obtain the 3-D vorticity equation:

$$\frac{\partial \xi}{\partial t} = \nabla \times (U \times \omega) + \nabla \times (bk) \qquad (9)$$

where $\omega = (\nabla \times U)$

Letting $\xi = k \bullet \omega$ to be the vertical component of vorticity and taking derivative of $\boldsymbol{k}$ from equation (9), we obtain the tendency equation of ξ in a non-rotating reference frame:

$$\frac{\partial \xi}{\partial t} = k \bullet \nabla \times (U \times \omega) \qquad (10)$$

from which we note that buoyancy only affects the horizontal vorticity components.

Taking the divergence of (8), we obtain a diagnostic equation for the disturbance pressure:

$$\nabla^2\left(\frac{p}{\rho_0}\right) = -\nabla^2\left(\frac{U \bullet U}{2}\right) + \nabla \bullet (U \times \omega) + \frac{\partial b}{\partial z} \qquad (11)$$

From equation (6), we see that there is a contribution to the dynamic pressure of equation (10) of the form:

$$\nabla \cdot \left(U' \times \overline{\omega}\right) = -\nabla \cdot \left(\omega' \overline{S}\right) \quad (12)$$

Using equation (11) the sign of the pressure perturbation due to this effect may be determined noting that:

$$\nabla^2 p_{dyn} \sim p_{dyn} \sim -\frac{\partial}{\partial x}\left(\omega' S_x\right) - \frac{\partial}{\partial y}\left(\omega' S_y\right) \quad (13)$$

This indicates that there is a positive dynamical pressure perturbation up-shear of the cell and a negative perturbation down-shear. In the case of unidirectional shear, the induced pressure pattern favors updraft growth of the leading edge of the storm. However, when the shear vector rotates clockwise with height, equation (13) shows a dynamical pressure disturbance pattern in which there is an upward directed vertical pressure gradient force on the flank of the cyclonically rotating cell and a downward directed pressure gradient force on the flank of the anticyclonic cell.

4. Hurricanes

Hurricanes develop from pre-existing tropical depressions that have somehow acquired a degree of circular symmetry and a warm/cold core, although such disturbances are rare. Also referred to as TCs and typhoons in some parts of the world, hurricanes are intense vertical storms developing over tropical oceans of very warm upwelling surface water and move around subtropical high. Although they are described in various terminologies in different parts of the world, they are basically similar types of storms. For example, some nomenclature exist such as in the NH (counterclockwise rotation): hurricane (Atlantic and East Pacific) –where they are classified by the damage they can cause [18]; typhoon (North Pacific); cyclone (North Indian Ocean) and SH (clockwise rotation): cyclone (South Pacific and South Indian Ocean). Typically, hurricanes have radial scales of several hundred kilometers similar to those of some midlatitude synoptic systems. They are well-organized spiral rain bands where the radial shear of swirling winds are large with high wave number are often dumped [43]. The triggering action is typically a tropical wave, its motion controlled by a deep layer of mean environmental flow [43]. The chief initiating mechanisms in the Atlantic is easterly waves [38]. Energy is derived from horizontal shearing motion in the easterlies and its core is cold because of dynamically induced lifting in the presence of weak horizontal temperature gradients [44].

Horizontal shear instability must be produced in the equatorial convergence zone; the locus of most easterly waves of this zone is located some distance off the equator and the converging air masses carry their angular momentum with them. A mature hurricane has different dynamical features (Fig. 5). Its center (called the eye) is surrounded by outwardly deep cloud known as the ‘eye wall.’ This is the region of increasing severity with heavy precipitation and strong swirling winds. Swirling in the core becomes strongly axisymmetric as the hurricane matures [19]. The eye is an area of relatively clear calm/fair weather sinking air, but warmest temperatures aloft, separated by an inversion [45]. Outside the eye wall are regions of loosely organized rainbands with a wide scale, often with convective cells.

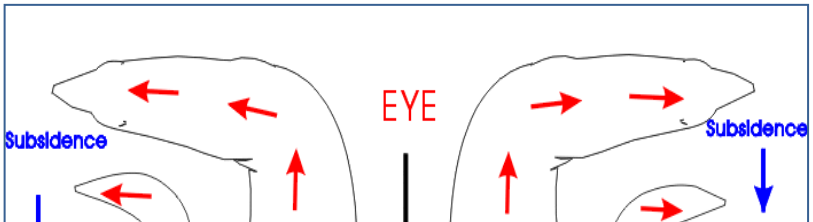

Fig. 5. Schematic-cross section of air circulation in a mature hurricane. Air spirals in towards the eye within the boundary layer, ascends along constant surfaces in the eye wall (red arrows), and subsides in the drier regions away from the eye wall (blue arrows). (https://www.hko.gov.hk/informtc/nature.htm).

Many factors affect tropical storm and hurricane activity over the North Atlantic; some of these show surprisingly strong long-range predictive signals for Atlantic basin seasonal TC activity up to 11 months in advance [46,47]. Another study by Gray and colleagues identified three prominent factors associated with this predictive skill: (1) the stratospheric QBO; (2) the ENSO cycle; and (3) West African rainfall. QBO describes a layer of winds that encircle the earth in the lower stratosphere, roughly between 20 and 40 km altitudes and 15° N and 15° S latitudes. The air masses alternate both easterly and westerly, reversing every 12-13th month. ENSO refers to the interaction between the atmosphere and ocean in the tropical Pacific, resulting in a periodic variation between below-normal and above-normal SSTs and dry/wet conditions over a few years. According to Gray et al. [48], the factors appear to be in a phase favorable for above normal Atlantic tropical activity by contributing to: (a) suppressed vertical wind shear across the subtropical North Atlantic between 10–20°N, and (b) a tendency for stronger easterly low-pressure waves (at approximately 15°N) which typically move across west Africa and propagate westward over the subtropical North Atlantic.

4.1. Balance in the pre-hurricane and tropical depression

In this context, the incipient hurricane is taken as a forced circulation driven by the heat released in the organized cumulus convection, not a free circulation driven by unbalanced buoyant forces [44]. Thus, the large-scale flow could be assumed as quasi-hydrostatic and discount unbalanced Coriolis and centrifugal forces, taking the horizontal forces to be approximately in a gradient state or geostrophic balance. The concept of balance is often used extensively in the analysis of large-scale gravitationally stable, extra-tropical motions. For example, applying the perturbation technique to small-

amplitude wave motions of a conditionally unstable saturated atmosphere, it is found that the small-scale modes grow at a greater rate and ultimately predominate. We can assume a pre-hurricane depression as sufficiently small horizontal scale so that we ignore the curvature of the earth and the variation of the Coriolis parameter.

The conditions for balance in the radial and vertical directions [44,49] may be written as:

$$-\rho\left(\frac{v^2}{r}+fv\right)-\frac{\partial p}{\partial r}=0 \qquad (14a)$$

$$-\rho g-\frac{\partial p}{\partial z}=0 \qquad (14b)$$

where p is pressure, ρ is air density, r is radial coordinate, z is counter clockwise tangential velocity component, f is the Coriolis parameter and g is gravitational field strength. Introducing perturbation analysis to equation (14a) reduces it to:

$$\rho fv-\frac{\partial p}{\partial r}=0 \qquad (14c)$$

Under weak assumption that the characteristic phase and orbital frequencies are small compared to the frequency of sound, it may be shown that the local and horizontal fluctuations of pressure, density and temperature are fractionally small. Taking horizontal density in space-time averages, equation (14a) may be approximated by:

$$\frac{\partial \chi}{\partial r}=\frac{m^2}{r^3} \qquad (14d)$$

where $\chi=\frac{(p-\bar{p})}{\bar{p}}+\frac{f^2r^2}{8}$ and m is the angular momentum per unit mass given by $m=rv+\frac{fr^2}{2}$

The continuity equation may also be approximated by:

$$\frac{\partial(\bar{\rho}ru)}{\partial r}+\frac{\partial(\bar{\rho}rw)}{\partial z}=0 \qquad (15)$$

where u is the radial velocity.

From equation (15), the divergence forms of the laws of conservation of angular momentum and energy may be written as:

$$\frac{\partial(\bar{\rho}rm^2)}{\partial t}+\frac{\partial(\bar{\rho}rum^2)}{\partial r}+\frac{\partial(\bar{\rho}rwm^2)}{\partial z}=0 \qquad (16a)$$

$$\frac{\partial(\bar{\rho}r\theta)}{\partial t}+\frac{\partial(\bar{\rho}ru\theta)}{\partial r}+\frac{\partial(\bar{\rho}rw\theta)}{\partial z}=\frac{\bar{\rho}r\bar{\theta}Q}{c_p\bar{T}} \qquad (16b)$$

where θ is potential temperature, c_p is specific heat capacity at constant pressure and Q is the rate of external heating per unit mass.

From equations (14a), (14c) and (16a), one notices that no frictional forces appear. This is because of the assumption that the entire effect of friction is confined to a surface boundary layer [44]. Although the turbulent moist-convective process which transports latent heat must also transport momentum and sensible heat both vertically and radially, these transports unlike friction in the surface layer, are essentially dissipative and can cut down the rate of swell development.

Although the wind and convective clouds observed in a hurricane are not very axisymmetric about the vortex center, the fundamental aspects of hurricane dynamics can be modeled by idealizing the hurricane as an axisymmetric vortex [42]. The thermal wind in an axisymmetric hurricane can be derived from the gradient wind balance cylindrical coordinates [43], expressed as:

$$\frac{V^2_\lambda}{r}+fv_\lambda=\frac{1}{\rho}\frac{\partial \Phi}{\partial r} \qquad (17)$$

where r is the radial distance from the centre (positive outward) and v_λ is the tangential velocity (positive for anticlockwise flow). It is sometimes useful to use the absolute angular momentum $M_\lambda=v_\lambda r+\frac{fr^2}{2}$ in place of v_λ

because above the boundary layer M_λ is nearly conserved following the air motion. In terms of M_λ the gradient wind balance can be expressed as:

$$\frac{M_\lambda^2}{r^3} - \frac{f^2 r}{4} = \frac{1}{\rho}\frac{\partial \Phi}{\partial r} \quad (18)$$

Eliminating Φ in equation (18) with the hydrostatic equation in log-pressure coordinates $\frac{\partial \Phi}{\partial z^*} = \frac{RT}{H}$ we obtain the relationship between the radial temperature gradient and the vertical shear of the absolute angular momentum

$$\frac{1}{r^3}\frac{\partial M_\lambda^2}{\partial z^*} = \frac{R}{H}\frac{\partial T}{\partial r} \quad (19)$$

where z is altitude, R is gas constant, H is the pressure height scale and T is air temperature. The cyclonic flow in a hurricane becames maximum near the top of the boundary layer. However, the inflow picks up latent heat through evaporation and exchanges sensible heat with the underlying ocean. Near the vortex center, the inflow turns upward and draws in latent heat from the boundary layer into the free atmosphere [19]. Dynamically, strong cyclonic swirling flow indicates strong inertial stability [43] given by:

$$I^2 = \left(f + \frac{2V_T}{r}\right)\left(f + \frac{1}{r}\frac{\partial r V_T}{\partial r}\right) \quad (20)$$

where V_T is tangential wind velocity. Because at the top of the boundary layer $\frac{\partial M_\lambda}{\partial z^*} < 0$, equation (19) implies that $\frac{\partial T}{\partial r} < 0$. Thus temperature maximum must occur at the center of the storm/hurricane. This is consistent with observation that hurricanes are 'warm core' systems.

The hurricane kinetic energy is maintained in the presence of boundary layer dissipation by conversion of latent heat required from the underlying ocean [42]. Conversely, potential energy is carried out by a transverse secondary circulation associated with the hurricane. Circulation consists of boundary layer inflow into a region of enhanced convection surrounding the eye wall ascent within convective cloud towers that tend to be concentrated in the narrow outward-sloping direction, radially out flow in a thin layer near the tropopause and gentle subsidence at a large radius. The water that evaporates from the sea surface into the inward flowing air within the boundary layer causes a large increase in the equivalent potential temperature θ_e, as the air approaches the aye wall [42]. Within the eye wall, potential temperature and absolute angular momentum surfaces coincide so that a parcel ascent in the eye wall neutralizes with respect to conditional instability, and does not require external forcing [42].

5. Monsoon circulations

The dynamical theories of thermally direct, zonally symmetrical circulations in the tropical atmosphere are reported in literature [50–52]. A summary from the findings is that below a certain threshold value of thermal forcing, the atmosphere maintains a steady state of thermal equilibrium. Beyond this threshold value, equilibrium breaks down and a meridional circulation is initiated. Effects of forcing on monsoon strength are due to changes in the amplitude of seasonal insolation and the resulting land-sea thermal and pressure contrasts [53], and references therein. The subtropical thermal forcing can be distinctively described for dry and moist atmospheres. For example, the moist atmosphere is more appropriate over tropical Africa relative to Sahel Africa. One important characteristic of moisture

transport in the atmosphere is residence time [54] -defined as the time spent by moisture in the atmosphere between evaporation and precipitation. This is also a fundamental balance in water cycle. Depending on the distribution of entropy, two possible regimes may dominate the dynamics in the tropics; a radiative-convective equilibrium regime or an angular momentum conserving regime [55]. The thermal wind can be expressed (for a zonally symmetrical atmosphere) as:

$$\frac{\partial u}{\partial p} = -\frac{1}{f}\frac{\partial \alpha}{\partial y} \quad (21)$$

where u is zonal wind, α is specific volume ($\alpha = 1/\rho$) and y is meridional distance.

Using Maxwell's theory, we can write:

$$\left(\frac{\partial \alpha}{\partial y}\right) = -\left(\frac{\partial \alpha}{\partial s}\right)_p \frac{\partial s^*}{\partial y} = \left(\frac{\partial T}{\partial p}\right)_s \frac{\partial s^*}{\partial y} \quad (22)$$

where s^* is saturation entropy given by $s^* = c_p \ln(\theta_e^*)$ and θ_e^* is equivalent potential temperature.

Besides the monsoon, there can exist other intraseasonal oscillations related to westerly bursts that modulate stability and wind shear near the equator [38]. For example the Madden-Julian Oscillation (MJO) is a large synoptic scale region that favours deep convection originating near east Africa and migrates eastwards, typically reaching its maxima over the Indian Ocean. Meridional monsoon circulation can develop over any tropical region (off the equator) when the absolute vorticity near the tropopause reaches a threshold value of zero. However, for a moist atmosphere satisfying a quasi-equilibrium balance between moist convection and the radiative forcing, absolute vorticity at the upper-tropospheric levels is a function of both latitude and the meridional distribution of boundary-layer entropy. Hence, the onset of a monsoon circulation depends in a nonlinear fashion on these two factors. But the monsoon is not controlled by simple land-sea thermal contrast only as zonal asymmetric diabatic heating and large-scale orography can also significantly affect it [56]. According to the authors, theory predicts that a flat distribution of entropy does not drive any circulation and that a relatively large gradient of entropy should strongly drive the monsoon circulation. A zero absolute vorticity in the upper troposphere is indicative of the presence of monsoon circulation [57].

A monsoon circulation is not simply driven by the east-west differential heating, but rather associated with the differential heating profile and maintained dynamically by the balance between a vorticity source and advection. The balance is reflected by a spatial quadrature relationship between the monsoon divergent circulation and the monsoon high/low at upper/lower levels [56], and references therein.

6. Long westerly waves

The atmosphere-land-ocean is a complex system supporting many different types of motions on a wide range, both spatially and temporally. For example, the huge cyclones and anticyclones have horizontal length scales, wave motion have periodic time scales in seconds, days or months [49]. In order to attempt a theoretical study of the atmosphere-ocean motions, we begin by identifying scales of motion interest to us and try to isolate important mechanisms because equations of motion are a very rich matrix from which a wide range of physical phenomena can occur. Among the phenomena permitted are the wave

motion and vorticity. Using the vorticity equation, and making additional assumptions of zero horizontal divergence purely horizontal flow autobarotropy, and neglecting additional forces, the vorticity equation may be expressed as:

$$\frac{d(\xi + f)}{dt} = 0 \qquad (23a)$$

or $$\frac{\partial \xi}{\partial t} + u\frac{\partial \xi}{\partial x} + v\frac{\partial \xi}{\partial y} + v\frac{\partial f}{\partial y} = 0 \qquad (23b)$$

where $\zeta = curl_z V = \frac{\partial v}{\partial x} - \frac{\partial u}{\partial y}$ is relative vorticity, **V** = (u,v) is velocity vector (assuming a 2-D fluid flow) and *u* and *v* are zonal and meridional velocity components. ζ is the vertical component of the 3-D vorticity vector ω, sometimes written as ω_z and is positive for counter-clockwise fluid rotation [58]. However, since ζ is usually smaller than *f* but greatest at the edge of fast currents, we normally use absolute vorticity ($\omega_a = \zeta + f$) which is the sum of planetary and relative vorticity.

A planetary wave may be studied within the framework of the Cartesian equation by making the so-called 'beta' or β-plane approximation [48]. β is the change in Coriolis force with latitude as a result of wave amplitude. The expression for β may be obtained from the Coriolis parameter *f*, noting that $f = 2\Omega\sin\phi$, whereupon $df/dy = 2\Omega\cos\phi \times d\phi/dy$.

Defining $\beta = \frac{\partial f}{\partial y} = \frac{2\Omega\cos\phi}{a}$ (where *a* is the earth radius) and assuming a broad westerly current of infinite lateral extent which is undulating north and south in a wave-like fashion, we may take the dependent variable to be independent of *y*. In this case, we deal with a system of waves in which the streamlines at any latitude are parallel to those at any other latitude. Thus $\zeta = \partial v/\partial x$, from which:

$$\frac{\partial^2 v}{\partial x \partial t} + u\frac{\partial^2 v}{\partial x^2} + \beta v = 0 \qquad (24)$$

We seek as a solution, waves which move in the *x*-direction with a constant speed *c*, without changing shape. Thus, if one follows a parcel moving in the east-west direction with speed *c*, no changes will be observed in any of the variables. Therefore, the operator $\frac{D}{Dt} = \frac{\partial}{\partial t} + c\left(\frac{\partial}{\partial x}\right) = 0$, where $\frac{D}{Dt}$ means individual derivative following an air parcel moving with speed *c*. Here $\frac{D}{Dt}$ is different from the operation $\frac{d}{dt}$ since the latter represents an individual derivative following an air parcel. With this assumption the vorticity theorem becomes:

$$(u - c)\frac{\partial^2 v}{\partial x^2} + \beta v = 0 \qquad (25)$$

Equation (24) is nonlinear because it involves a product of dependent variables and is therefore not easy to solve. We may apply the perturbation method in order to reduce it to a linear differential equation. For example, we assume the horizontal flow to be made up of a large basic current *U* (the zonal wind component), with a west-east flow upon which are superimposed small variable perturbations u' and v',which are functions of distance *x* and time *t*. Thus;

$$u(x,t) = U + u'(x,t)$$
$$v(x,t) = v'(x,t)$$

Here *U* is considered to be a quantity of zero-order magnitude, while u' and v' (which are one step smaller) are of the first order magnitude. If one adopts a log scale to base ten, then u' and v' will be about one-tenth as large as *U*, so that equation (25) becomes:

$$(U-c)\frac{\partial^2 v}{\partial x^2}+\beta v'+u'\frac{\partial^2 v'}{\partial x^2}=0 \qquad (26)$$

The first two terms are first order in size while the last term consists of the product of two first-order quantities and hence the second order in magnitude. Within this degree of precision, the second-order term can be neglected so that equation (26) reduces to a linear equation of the form:

$$\frac{\partial^2 v'}{\partial x^2}+\frac{\beta}{(U-c)}v'=0 \qquad (27)$$

Since x is the only independent variable, this corresponds to an ordinary second-order differential equation with constant coefficients. Solution for v' is known to be sinusoidal in x. To show this we can use a trial solution of the form

$$v'=v_0\sin\frac{2\pi x}{L} \qquad (28)$$

where v_0 is a constant amplitude and L is the wavelength. Substituting this into equation (26) yields:

$$U-c=\frac{\beta L^2}{4\pi^2} \qquad (29)$$

Equation (29) is a relationship existing between the wave speed and wavelength of sinusoidal waves if equation (27) is to be satisfied. Such an expression of wave phenomena is called the *frequency equation*. One can see that when c is positive (waves progress from west to east) $U - c$ is smaller than U and the wavelengths are relatively short. When c is negative (waves retrogress from east to west), $U - c$ is larger than U and the wavelengths are relatively long. Upper-level waves in the westerlies in midlatitudes usually move from west to east as a result of advection (a process in which the airflow transports a property of the atmosphere downstream) and in part as a result of propagation, which acts in the opposite direction towards the west. From equation (29) the phase speed of the waves can be expressed as:

$$c=U-\frac{\beta L^2}{4\pi^2} \qquad (30)$$

where U is speed from west to east of the component of the upper-level wind due to uniform flow, β is the meridional or north-south gradient of the Coriolis parameter. Since the magnitude of f increases towards the poles, β is positive and hence waves with shorter wavelengths have a relatively small component due to propagation. Under this condition, advection overwhelms the effect of propagation and waves move downstream. On the other hand, if in the midlatitudes the wavelength is long, effects of propagation may cancel those of advection and waves may become stationary or retrograde. The wavelength of stationary waves occurs when $c = 0$, from which equation (30) yields:

$$L_s=2\pi\sqrt{\frac{U}{\beta}} \qquad (31)$$

7. Jet streams and wave tracks

When the longitudinally asymmetric geopotential anomalies associated with stationary waves are added to the zonal-mean geopotential distribution, the resulting time mean field includes local regions of enhanced meridional potential gradient that are manifested in the wind field of the NH by the Asian and north American jet streams. In addition to the two jet cores in West Pacific and West Atlantic, there is also a third jet core centered over North Africa, although it is weaker than the two [59]. To understand the momentum budget in the jet streams and its relationship to weather distribution, we consider the zonal component of the momentum equation

$$\frac{D_g u_g}{Dt}-f_0(v-v_g)=f_0 v_a \qquad (32)$$

where v_a is the meridional component of the ageostrophic wind. This equation

indicates that the westerly acceleration $(D_g u_g/Dt > 0)$ that air parcels experience as they enter the jet can only be provided by a poleward ageostrophic wind component $(v_a > 0)$ and conversely acceleration that air parcels experience as they leave the jet requires an equatorward ageostrophic motion. This meridional flow with accompanying vertical circulation is illustrated in figure below.

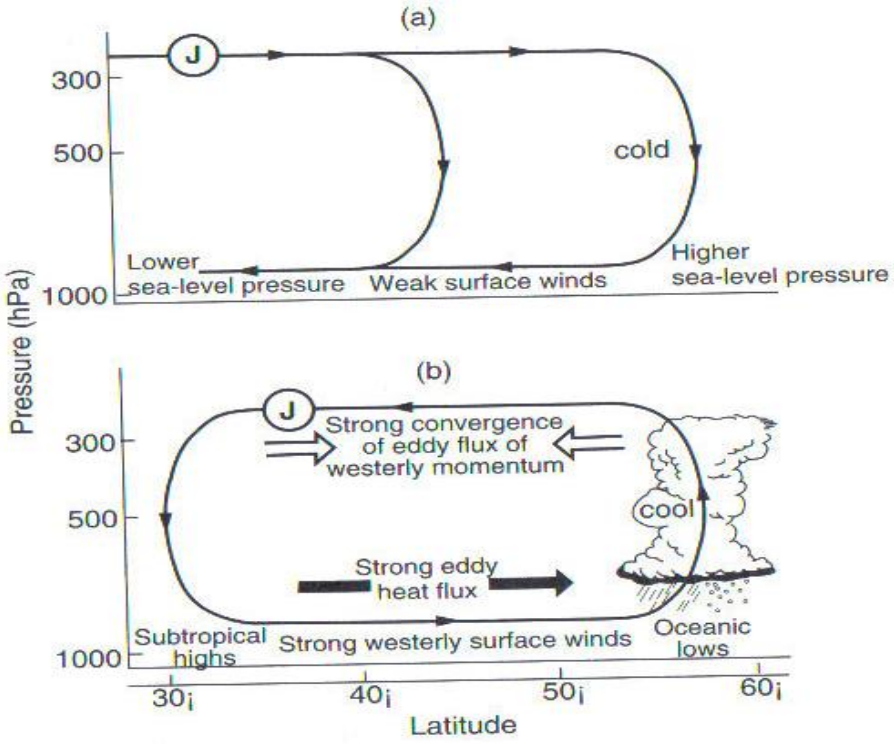

Fig. 6. Meridional cross sections showing the relationship between the time mean secondary meridional circulation (continuous thin lines with arrows) and the jet stream (denoted by J) at locations upstream & downstream from the jet stream cores [42].

Downstream of the jet core however, the secondary circulation is thermally indirect, but much stronger than the zonally averaged Farrell cell. Because the growth rate of baroclinically unstable synoptic scale disturbances is proportional to the strength of the basic state thermal wind, it would not be surprising that the Pacific and Atlantic jet streams can be important SRs for storm development. This jet mode appears to be forced by anomalous tropical heating associated with the ENSO cycle and intra-seasonal variability such the MJO [60], and references therein. Synoptic waves travel along the subtropical jet over the South Indian Ocean in the region of strongest surface westerly winds [60] and south of Australia [61]. When the waves propagate equatorward into the westerly dust in the upper troposphere over equatorial Pacific they trigger deep

convection [62]. Typically transient baroclinic waves develop in the jet entrance region and grow as they are advected downstream and decay in the jet exit region. The African Easterly Jet (AEJ), also popularly called the Somali Jet can be viewed as a western boundary current of the East African highlands. This is normally observed over North Africa [63], and occurs due to the reversed surface temperature gradient when the Sahara becomes hotter than the equatorial regions [38,64]. The jet flow develops from instabilities over sub-Saharan Africa [34]; its origin lies over the Indian Ocean in the form of southeast trades. However, trades tend to be more from an east-southeast direction than their name implies. A steady zonally symmetric solution indicates that the combination of inertial forces, surface friction and weak subsidence provide adequate ingredients of the southeast trades over the South Indian Ocean [65].

The AEJ plays a crucial role than the intertropical convergence zone (ITCZ) and generally linked to the well-organized mesoscale features [66] in the rainfall production by triggering atmospheric disturbances at its southern and northern boundaries. Some emerging theory also relates the formation of such atmospheric disturbances in the vicinity of the AEJ to a barotropic-baroclinic energy conversion process [67,68]. The wind regime in northwest Africa is dominated by the north to north-easterly trades that blow on the eastern flank of the quasi-permanent anticyclone in the North Atlantic (the 'Azores' high). These winds are stronger and tend to move towards the northwest during the NH summer (May–September). Equatorial West Africa generally has light winds with diurnal sea breezes. However, there is a weak monsoon effect in the Gulf of Guinea, which means continuous onshore winds between June and August. Relatively cool moist air from the Gulf of Guinea is often advected onto the warm dry continental landmass where the resulting rainband can travel from the coast to Sahel and back again, following the movement of the ITCZ [69].

Several other studies have been conducted on tropical African waves and cyclogenesis [14,70–73]. Most of these studies outline the climatology of African easterly waves (AEWs) and their propagation over African and global environment. AEWs are synoptic-scale tropical disturbances that form over northern Africa [74] and propagate westwards as unbroken progressions across Africa and the Atlantic Ocean during summer [71–73]. They move in trade wind belt and occur most frequently in August–September between 5° and 20 °N and appear to be breeding grounds for hurricanes. They are a fundamental component of the west African climate [75] and commonly known as the main precursors of TCs in the Atlantic [72,76]. It is estimated that they account for 60% of the Atlantic tropical storms and about 85% of the major hurricane activity [14,63]. The north wave primarily grows in association with dry baroclinic energy conversions at the southern margin of the Sahara, while southern-track mainly result from barotropic instability and interactions with deep conversion [73], and references therein. The southward track is driven by barotropic-baroclinic energy conversion and can exhibit stronger circulation over West Africa [72]. Although it has been hypothesized, for decades that AEW generation was

due to a mixed baroclinic-barotropic instability of the AEJ, recent studies now indicate that baroclinic and barotropic conversions from these instabilities alone do not account for the AEW growth. The triggering mechanisms are the mesoscale convection and upstream development from the previous AEW [74,77].

Along the southwest coast, predominant winds are south or south-easterly trades, and strongest during southern summer (October–April). The more southerly regions are often influenced by the mid-latitude depressions during southern winter, and so winds are often stormy and appear to come from a westerly quarter. However, during summer, the south-easterly trades predominate. In the Cape Peninsular, with virtually no land topography, these winds can reach strong to gale force [78]. Over east Africa, winds are predominantly from north or northeast, whereas over southern Africa, the influence of mid-latitude weather systems means the possibility of winds from a south-westerly quarter during winter. Much of the east-coast which is out of the influence of cold currents and up-welling is generally warm, with greater seasonal variation further south. In the trade-wind belts of the northwest and southwest Africa there is up welling. Oceanic upwelling occurs mainly as a result of surface water divergence due to wind stress so that adjacent surface does not flow back, obstructed by the landmass in the upwind direction [60]. This, together with the proximity of cold, equatorward-flowing currents means that the water can be uncharacteristically cold for the latitude. For example, the western part of South Africa is renowned for episodic up welling events associated with the Cape Doctor [78].

8. Conclusion

The global distribution of continental landmasses is a major factor determining the nature of swells on the global wave climate. However, the relative importance of remote forcings on the African climate remains a key area of uncertainty [12]. For example, there is considerable uncertainty at the regional scale whether TC numbers may decrease or increase, or whether SRs will remain the same. Despite the presence of massive land barriers, extratropical swells from the NH can also contribute significantly to the wave activity in remote locations, in addition to tropical environment-generated waves. This demonstrates that the earth's climate was and will possibly never be in equilibrium [79]. Nevertheless, climate science has been active in taking advantage of advances in basic mathematical and physical approach to provide simulations to address new fundamental problems [80]. In the present study, we use the so-called Navier-Stokes equations to understand the swell dynamics around Africa. The study gives motivation to the climatological pattern of wave activity and swell propagation characteristics as primarily related to the main sea state and wind patterns and may also help improve extreme weather predictions and monitoring.

There are key concepts to note: tropical waves play an important role in the formation of large scale sea breezes which frequently take shape over Africa; south-east African region is known for frequent occurrence of extreme waves and is a challenging one for wave forecasting. The climatological distribution of these waves can largely

be weighted by storm waves coming from the southern oceanic areas, giving rise to statistical signature in wave-current interactions across Africa. Just like in most parts of the world where the development and behaviour of such systems is critical, given their potential impacts, these need to be closely watched over southern Africa [10]. This is very crucial since the sub-region frequently experience such events, often accompanied by devastating impacts. Also, there are two important factors which tend to be linked with an active Atlantic hurricane season. First, the westerly phase of the stratospheric QBO, which can reach peak amplitude and contribute to low vertical wind shear throughout the subtropical North Atlantic. Second, above-normal rainfall over the Gulf of Guinea can favor enhanced soil moisture and may contribute to development of the West African rainy season, and subsequently stronger easterly low-pressure waves. Also noteworthy is the combination of ENSO and the Atlantic SST anomalies which may give rise to complex wind flow changes in the near-equatorial Atlantic. Factors such as characteristics of the moist layer, position and/or the intensity of the ITCZ may also play a role in the link between inter-decadal and inter-annual variability and wave activity. Lastly, it is clear that atmospheric waves are linked to large-scale shifts in climate and can change systematically at the longest time scale.

Competing Interests

The author has declared no competing interests

References

1. Mather A, Stretch DD. A perspective on Sea Level Rise and Coastal Storm Surge from Southern and Eastern Africa: A Case Study Near Durban, South Africa. Water. 2012; 2, 237-259; doi:10.3390/w4010237.
2. World Meteorological Organization. 2001–2010. A Decade of Climate Extremes. 2013; URL: https://library.wmo.int/pmb_ged/wmo_1103_en.pdf
3. Lutjeharms JRE, Monteiro PMS, Tyson PD, Obura D. The oceans around southern Africa and regional effects of global change. South African journal of Science 97, 2001; March/April 2001, 119.
4. Wiston M, Mphale KM. Mesoscale Convective Systems: A Case Scenario of the 'Heavy Rainfall' Event of 15–20 January 2013 over Southern Africa. Climate. 2019; 7, 73; doi:10.3390/cli7060073., www.mdpi.com/journal/climate
5. Fitchett JM, Grab SW. A 66-year tropical cyclone record for south-east Africa: temporal trends in a global context. Int. J. Climatol. 2014; **34**: 3604–3615 (2014), doi: 10.1002/joc.3932.
6. Hall R, Erdélyi R, Hanna E, Jones JM, Scaife AA. Drivers of North Atlantic Polar jet stream variability. Int. J. Climatol. 2014; doi::10.1002/joc.4121
7. Rowell S, Weather, Current and Routing Brief. The Clipper 11/12 Round the World Race. 2011; URL: http://rowellyachtingservices.com/media pool/93/937691/data/Clipper_11_12_brief.pdf.
8. Quilfen Y, Yurovskaya M, Chapron B, Ardhuin F. Storm waves focusing and steepening in the Agulhus current: Satellite observations and modeling. Remote Sensing Environment. 2018; 216 (2018) 561–571.
9. Millner A, Washington R. What determines perceived value of seasonal climate forecasts? A theoretical analysis.

Global Environmental Change. 2010; www.elsevier.com/locate/gloenvcha
10. Moyo EN, Nangombe S. Southern Africa's 2012-13 Violent Storms: Role of Climate Change. 2015; Porcedia IUTAM 17 (2015) 69–78.
11. Woodroffe CD. Coasts: Form, Process and Evolution. 2002; Cambridge University Press.
12. Zaitchik BF, Levin NE. Understanding the Dynamics of the Tropical African Climate. 2013; Workshop on Climate Dynamics of Tropical Africa; Baltimore, MD, 15–16 November 2012. EOS, 2013; Vol. 94, No. 23.
13. Bhowmick SA, Kumar R, Chaudhuri S, Sarkar A. Swell Propagation over Indian Ocean Region. Int. J. Ocean Clim. Sys., 2011; 2(2), 87–99.
14. Landsea CW. A climatology of intense (or major) Atlantic hurricanes. Mon. Wea. Rev., 1993; 121, 1703–1713, doi:10.1175/1520-0493(1993)121,1703:ACOIMA.2.0.CO;2.
15. Rossouw M, Terblanche L, Moses J. General Characteristics of long Waves around the South African Coast. 2013; Stellenbosch, South Africa. CSIR.
16. Gray WM. Tropical cyclone genesis. Colorado State University Department of Atmospheric Science Paper No. 234. Colorado State University: Fort Collins. 1975;1–121.
17. Shultz JM, Shephered JM, Bagrodia R, Espinel Z. Tropical cyclone in a year of rising global temperatures and a strengthening El Nino. Disaster Health Briefing., 2014; hhp://dx.doi.org/10.10802165044.2012.1111722
18. Holton JR, Pyle J, Curry JA. Encyclopedia of Atmospheric Sciences. 2003; URL: https://www.atmos.umd.edu/~nigam/Encyc.Atmos.Sci.Stationary.Waves.Nigam-DeWeaver.2003.pdf
19. Marks FD. Hurricanes. Hurricane Research Division. 2003; URL: http://curry.eas.gatech.edu/Courses/6140/ency/Chapter11/Ency_Atmos/Hurricanes.pdf
20. Vethamony P, Rashmi R, Aboobacker VM. Recent studies on wind seas and swells in the Indian Ocean: a review. 2013;Vol. 4, November 1, https://journals.sagepub.com/doi/pdf/10.1260/1759-3131.4.1.63
21. Joubert JR, van Niekerk JL. South African Wave Energy Resources Data: A case study. Center for Renewable and Sustainable Energy Studies. 2013; URL: https://www.crses.sun.ac.za/files/research/publications/technical-reports/SANEDI(WaveEnergyResource)_edited_v2.pdf
22. Forristall GZ, Ewans K, Olagnon M, Prevosto M. The West Africa Swell Project (WASP). Proceedings of the 32nd International Conference on Ocean, Offshore and Arctic Engineering. OMAE2013. 2013; June 9–14. Nantes, France.
23. Thurman HV, Trujillo AP. Waves and Water Dynamics. Chapter 8. Essentials of Oceanography. 2001; 7th Ed. Prentice Hall, Indiana.
24. Wang Z, Montgomery MT, Fritz C. A First Look at the Structure of the Wave Pouch during the 2009 PREDICT-GRIP Dry Runs over the Atlantic. Mon. Wea. Rev. 2012; 140, 1144–1163.
25. Alves JHGM. Numerical modeling of ocean swell contributions to the global wind-wave climate. Ocean Modelling., 2005; www.elsevier.com/locate/ocemod
26. Fan Y, Griffiths MS, Lin SJ, Hemer M. Simulated Global Swell and Wind-Sea Climate and Their Responses to

Anthropogenic Climate Change at the End of the Twenty-First Century. Journal of Climate. 2014; Vol. 27., pp 3516–3536.
27. Freias EGG, Lorenzzetti JA, Chapron B. Swell and Wind-Sea Distributions over the Mid-Latitude and tropical North Atlantic for the Period 2002-2008. International Journal of Oceanography. 2012; Vol. 2012, Article ID 306723., hhp://dx.doi.org/10.1155/2012/306723
28. Carrrasco A, Semedo A, Isachsen PE, Christensen KH, Saetra Ø. Global surface wave drift climate from ERA-40: the contributions from wind-sea and swell. Ocean Dynamics, 2014; Vol. 64, Issue 12, pp. 1815–1829.
29. Reddy-Davis CL, Vincent K. Climate Risk and Vulnerability: A Handbook for Southern Africa. 2017; (2nd Ed), CSIR, Pretoria, South Africa. ISBN 978-0-620-76522-0
30. Lesolle D. Adaptation to Global Warming and Resulting Climatic Changes. 2004; 2nd AIACC Workshop, 24–27. Dakar, Senegal.
31. World Meteorological Organization. Edition. Annual Summary of Global Tropical Cyclone Season. 2000; WMO/TD-No. 1082. Report No. TCP-46. URL: https://library.wmo.int/pmb_ged/wmo-td_1082_en.pdf
32. Reason CJC, Keibel A. Tropical Cyclone Eline and Its Unusual Penetration and Impacts over the Southern African Mainland. Weather Forecasting. 2004;Vol. 19, pp. 789–805.
33. Kadomura H. Climate anomalies and extreme Events in Africa in 2003, including heavy rains and floods that occurred during northern hemisphere summer. African Study Monographs, Suppl. 2005;30:165–181, March 2005.
34. Barbosa HA. The African Easterly Waves and their influence on hurricane activity in the tropical North Atlantic: An assessment of hurricane Bill (2009) using SERVIRI data. 2018; CWG Workshop, 17–19 April 2018, Ljubljana, Slovenia.
35. Trapp RJ. Formation and development of convective storms. In: Oxford Research Encyclopedia of Climate Science (Ed. H. Storch). 2018; Oxford University Press, Oxford.
36. Weisman MJ, Klemp JB. Characteristics of Isolated Convective Storms. In: ray P.S. (eds) Mesoscale Meteorology and Forecasting. American Meteorological Society. 1986; Boston, MA., https://doi.org/10.100.
37. Neto CPS, Barbosa HA, Beneti CA. A. A method for convective storm detection using satellite data. Atmósfera. 2016; 29, 343–358.
38. Barnes GM. Meteorological hazards in the Tropics: severe convective storms and flash floods. In *Tropical Meteorology, Encyclopedia of Life Support Systems (EOLSS)*. 2010; p. 109, UNESCO, Paris, France, http://www.eolss.net.
39. Dotzek N, Groenemeijer P, Feuerstein B, Holzer AM. Overview of ESSL's severe convective storms research using the European Severe Weather Database ESWD. 2008.
40. LaCasce JH. Atmosphere-Ocean Dynamics. E-book. 2013; URL: https://www.uio.no/studier/emner/matnat/geofag/nedlagte-emner/GEF4500/h13/gef4500jhl6.pdf
41. Johnson RH, Mapes BE. Chapter 3: Mesoscale Processes and Severe Convective Weather. In Severe Convective Storms by Charles A. Doswell. Meteorological Monographs, 2011;E-book.

42. Holton JR. An Introduction to Dynamic Meteorology. 2004. Elsevier Press.
43. Wang Y. Hurricane Dynamics. Encyclopedia of Atmospheric Sciences, 2nd Ed. 2016; Vol. 6., http://dx.doi.org/10.1016/B978-0-12-382225-3.00488-6
44. Charney JG, Eliassen A. On the Growth of the Hurricane Depression. Journal of the Atmospheric Sciences. 1963;Vol 21, No 1. pp 68–75. American Meteorological Society.
45. Willoughby HE. Tropical Cyclone Eye Thermodynamics. Mon. Wea. Rev. 1998;126, 3053–3067.
46. Gray WMCW, Landsea PW, Mielke Jr., Berry KJ. Predicting Atlantic Seasonal Hurricane Activity 6–11 Months in Advance. Weather Forecasting. 1992;7, 440–455.
47. Gray WMCW, Landsea PW. Mielke Jr., Berry KJ. Predicting Atlantic Basin Seasonal Tropical Storm Activity by June 1. Wea. Forecasting. 1994a; 9, 103–115.
48. Gray WMCW, Landsea PW, Mielke Jr., Berry KJ. Extended Range Forecasting of Atlantic Seasonal Hurricane Activity for 1995, as of 30 November 1994. Department of Atmospheric Sciences, Colorado State University. 1994;Fort Collins, CO, 9 pp.
49. Smith RK. Lectures on Dynamical Meteorology. e-book. Version: June 16. 2014; URL: https://www.meteo.physik.uni-muenchen.de/~roger/Lectures/Dm_Lectures/DM_2014.pdf
50. Dickinson R, Henderson-Sellers A, Kennedy P, Wilson M. Biosphere-Atmosphere Transfer Scheme (BATS) for the NCAR community climate model. 1986; NCAR Tech Note, NCAR/TN-275+STR.
51. Emanuel KA. On thermally direct circulations in moist atmospheres. Journal of the Atmospheric Sciences.1995;52 (15), 1529–1534.
52. Jury MR, Enfield DB, Mélice JL. Tropical monsoons around Africa: Stability of El Niño-Southern Oscillation associations and links with continental climate. J. Geophy. Res., 2002;107. No. 0., doi: 10.1029/20000JC000507.
53. Zhisheng A. et al. Global Monsoon Dynamics and Climate Change. *Annu. Rev. Earth Planet. Sci.* 2015;**43**, 29–77 (2015).
54. Läderach A, Sodemann H. A revised picture of the atmospheric moisture residence time. Geo. Res. Lett., 2016; doi: 10.1002/2015GL067449
55. Plumb RA, Hou AY. The response of a zonally symmetric atmosphere to subtropical thermal forcing: Threshold behavior. J. Atmos. Sci., 1992;49, 1790–1799.
56. Wu G, Liu Y, Dong B, Liang X, Duan A, Bao Q, Yu J. Revisiting Asian monsoon formation and changes associated with Tibetan Plateau forcing: I. Formation. Clim Dyn. 2012;39:1169–1181., doi: 10.1007/s00382-012—1334-z
57. Cook KH. Large-Scale Atmospheric Dynamics and Sahelian Precipitation. Atmospheric Science Program, Cornell University, Ithaca, N. Y., Journal of Climate. 1996;pp. 1137–1152.
58. Van de Berg WJ. Potential vorticity: the swirling motion of geophysical fluids. Chapter 12. 2018; Vorticity in the Ocean.
59. Christenson CE, Martin JE, Handlos ZJ. A Synoptic Climatology of Northern Hemisphere, Cold Season Polar Subtropical Jet Superposition Events. Journal of Climate. 2017;Vol. 30, pp. 7231–7246

60. Shulmeister J, Goodwin I, Renwick J, Harle K, Armand L, Mcglone MS, Cook E, Dodson J, Hesse PP, Mayewski P, Curran M. The Southern Hemisphere westerlies in the Australasian sector over the last cycle: a synthesis. Quaternary International Journal. 2004;118–119 (2004) 23–53.
61. Stan C, Straus DM, Frederiksen JS, Lin H, Maloney ED, Schumacher C. Review of tropical-extratropical teleconnections on intraseasonal timescales. Reviews of Geophysis. 2017;55. https://doi.org/10.1002/2016RG000538.
62. van der Wiel K, Matthews AJ, Joshi MM, Stevens DP. The influence of diabatic heating in the South Pacific convergence zone on Rossby wave propagation and the meanflow. Quarterly Journal of the Royal Meteorological Society. 2016;142, 901–910. https://doi.org/10.1002/qj.2692
63. Lin YL, Liu L, Tang G, Spinks J, Jones W. Origins of the pre-tropical storm Debby (2006) African easterly wave-mesoscale convective system. Meteorol Atmos Phys. 2013; doi: 10.1007/s00703-013-0248-6.
64. Ferreira RN, Rickenbach T, Williams E, Guy N. African Easterly Waves and Atlantic Hurricanes. 2009; URL: http://www.ecu.edu/renci/floyd/slides/Floyd_B07_African-Waves.pdf
65. Bannon PR. On the Dynamics of the East African Jet I. Simulation of the Mean Conditions for July. Journal of Atmospheric Sciences. 1979; Vol. 36, Issue II. pp 2139–2152. American Meteorological Society. URL:https://www.essl.org/media/cwg/44.pdf
66. Grist J P, Nicholson SH. Easterly Waves over Africa. Part II: Observed and Modeled Contrasts between Wet and Dry Years. Mon. Wea. Rev., 2001; 130: 212–225.
67. Hagos SM, Cook KH. Dynamics of the West African monsoon jump. J. Clim. 2007;20:5264–5284. doi: 10.1175/2007JCLI1533.1
68. Cornforth RJ, Hoskins BJ, Thorncroft CD. The impact of moist processes on the African easterly jet–African easterly wave system. Q J R Meteorol Soc. 2009; 135:894–913. doi: 10.1002/qj
69. Klein C, Heinzeller D, Bliefernicht J, Klunstmann H. Variability of West African monsoon patterns generated by a WRF multi-physics ensemble. Clim Dyn. 2015; 45:2733–2755, doi: 10.1007/s00382-015-2505-5
70. Thorncroft CD, Hodges K. African easterly wave variability and its relationship to Atlantic tropical cyclone activity. J. Climate. 2001;**14**, 1166–1179.
71. Burpee RW. Characteristics of African Easterly Waves. In: Johnson R.H., Houze R.A. (eds) A Half Century of Progress in Meteorology: A Tribute to Richard Reed. Meteorological Monographs. American Meteorological Society. 2003; Boston, MA, doi:https://doi.org/10.1007/978-1-878220-69-1_7
72. Skinner CB, Diffenbaugh NS. *Projected changes in African easterly wave intensity and track in response to greenhouse forcing. Proc. Natl Acad. Sci. USA. 2014; **111**, 6882–6887.*
73. Dieng A L, Sall SM, Eymard L, Leduc-Leballeur M, Lazar A. Trains of African easterly waves and their relationship to tropical cyclone genesis in the eastern Atlantic. Mon. Wea. Rev., 2017;145, 599– 616, http://doi.org/10.1175/mwr-d-15-0277.1.
74. Bain CL, Parker DJ, Dixon N, Fink AH, Taylor CM, Brooks B, Milton SF.

Anatomy of an observed African easterly wave in July 2006. Q. J. R. Meteorol. Soc. 2011;137:923–933. Doi:10.1002/qj.812
75. Burpee RW. Characteristics of North African easterly waves during the summers of 1968 and 1969. J. Atmos. Sci., 1974;31, 1556–1570.
76. Pasch RJ, Avila LA, Jiing JG. Atlantic tropical systems of 1994 and 1995: A comparison of a quiet season to a near-record-breaking one. Mon. Wea. Rev., 1998;126, 1106–1123,doi:10.1175/1520-0493(1998)126,1106:ATSOAA.2.0.CO;2.
77. White JD. Mechanisms of African Easterly Wave Genesis. 2018;URL: https://ams.confex.com/ams/33HURRICANE/webprogram/Paper339214.html.
78. Kruger AC, Golinger AM, Retief JV, Sekele S. Strong wind climatic zones in South Africa. Wind and Structures, 2010;Vol. 13, No. 1.
79. Ghil M, Chekroun MD, Simonnet E. Climate dynamics and fluid mechanics: Natural variability and related uncertainities. Physica D: Nonlinear phenomena, Special Issue on the Euler Equations: 250 Years On, {\bf 237}. 2010; doi:10.1016/j.physd.2008.03.036
80. Lucarini V, Blender R, Herbert C, Ragone F, Pascale S, Wouters J. Mathematical and physical ideas for climate science. Reviews of Geophysics. 2014;doi: 10.1002/2013RG000446.